

## Calculation of adiabatic and diabatic $^3\Sigma^-$ states of $\text{OH}^+$

J A Spirko, J T Mallis and A P Hickman

Department of Physics, Lehigh University, Bethlehem, PA 18015, USA

Received 17 February 2000, in final form 10 April 2000

**Abstract.** Electronic structure calculations for several  $^3\Sigma^-$  states of  $\text{OH}^+$  are reported. These states are important for the charge-exchange process  $\text{O} + \text{H}^+ \leftrightarrow \text{O}^+ + \text{H}$ . Diabatic potential curves and their couplings were determined using the methodology of Pacher *et al* and of Domcke and co-workers, which is based on CAS-MCSCF-CI calculations followed by block diagonalization. The dimension of the matrix representation of the diabatic Hamiltonian is determined by  $N_\alpha$ , the number of interacting states included in the block diagonalization. Suitable values for  $N_\alpha$  depend on the internuclear separation, and several alternatives are compared. Further analysis of the calculations indicates that the excited oxygen ( $2p^3 3s \ ^3S$ ) level participates in charge exchange through a two-step mechanism not previously recognized: Stark mixing of oxygen levels by a distant proton leads to an admixture of  $2p^4$  and  $2p^3 3s$  configurations, and the diffuse  $3s$  orbital then provides the dominant coupling with the  $\text{O}^+ + \text{H}$  state.

### 1. Introduction

The charge exchange reaction of oxygen with the hydrogen ion and the reverse process are important in the upper atmosphere and in the interstellar medium [1–3]. One may represent these reactions simply as



However, a careful analysis of the process must explicitly include the fine structure levels of the oxygen atom ( $^3P_J$ ,  $J = 2, 1, 0$ ), because of the near degeneracy (within  $0.1 \text{ cm}^{-1}$ ) of the asymptotic limit  $\text{O}(^3P_1) + \text{H}^+$  with the alternative charge state  $\text{O}^+(^4S_{3/2}) + \text{H}$ . This feature places exceptional demands on the theoretical description of the scattering process, for several reasons. First, the well established theory of fine-structure mixing [4–7] must be generalized to include the additional channels of charge exchange. Second, the potential curves used in the calculations, which are usually first determined in  $LS$  coupling, must have accurate asymptotic limits since they determine the spacings of the fine-structure levels. Finally, the charge-exchange coupling must be calculated. In practice this means that either radial coupling matrix elements between adiabatic states must be calculated, or a ‘diabatic’ representation of the electronic Hamiltonian must be determined.

Various workers have addressed these issues. Several calculations of potential curves for the  $\text{OH}^+$  system have appeared in the literature over the years. Liu and Verhaegen [8] presented semi-empirical curves, and Saxon and Liu [9] performed MCSCF-CI calculations. Neither of these calculations provided the coupling terms necessary to treat charge exchange. Chambaud *et al* [10] formulated a theory combining fine-structure excitation with charge exchange and used estimated coupling terms to perform coupled channel scattering calculations. Recently Kimura *et al* [11] reported potential curves and radial coupling matrix elements, and Stancil

*et al* [12] used them for scattering calculations. The results of Stancil *et al* [12] differ substantially from those of Chambaud *et al* [10] for energies less than about 0.1 eV. Two of the present authors have also reported preliminary coupled channel calculations, using older potential curves [13].

In this paper we report new calculations of the lowest  $^3\Sigma^-$  potential curves and their couplings, which are the most critical for charge exchange. Our work takes advantage of a great deal of effort in recent years related to the direct calculation of ‘diabatic’ potential curves [14–19]. We have implemented, with some refinements, the approach of Domcke and co-workers [16, 18]. Carefully defined molecular orbitals (MOs) are used to calculate a CAS-MCSCF-CI wavefunction and set up a large matrix representation of the electronic Hamiltonian  $H$ . We then block diagonalize the Hamiltonian using the technique of Pacher *et al* [14] to provide a diabatic representation of  $H$ .

Our application to  $\text{OH}^+$  is complementary to the work of Kimura *et al* [11], because we avoid the radial coupling matrix elements entirely and calculate the diabatic Hamiltonian independently at each  $R$ . There is no need to propagate the results from one value of  $R$  to the next. The method we use is also well suited to the case where the spacing of the energy levels is critical, because the asymptotes of the diagonal diabatic curves can be adjusted independently of the coupling terms between them.

Several interesting features have emerged in the course of our calculations. We have found that excited states of the  $\text{OH}^+$  molecule play a crucial role in the charge exchange. Briefly, the  $\text{O}(2p^4\ ^3P)$  state of oxygen is effectively mixed with the excited  $\text{O}(2p^33s\ ^3S)$  by the  $\text{H}^+$  due to the Stark effect. In the asymptotic region ( $R \rightarrow \infty$ ) a small admixture of the 3s oxygen configuration in the multi-configuration wavefunction makes the dominant contribution to the charge-exchange coupling. This result means that our calculated charge-exchange coupling is about a factor of two larger asymptotically than the result used by Chambaud *et al* [10], who did not consider the Stark mixing.

This paper is organized as follows. Section 2 discusses the theory. The electronic structure methods implemented for the calculation of diabatic potential curves are summarized, and the details of our application to  $\text{OH}^+$  are given. Section 3 presents and discusses our results, and section 4 gives concluding remarks.

## 2. Theory

### 2.1. Determination of diabatic potential curves

In 1993, Domcke *et al* [16] observed that the state averaged CAS-MCSCF method of electronic structure calculation was well suited to calculating MOs appropriate for diabatic representations. The MCSCF method [20] involves expressing the electronic wavefunction  $\Psi(R)$  (in  $LS$  coupling) as a sum of configuration state functions (CSFs)  $\Phi_i$  that have the desired spin and orbital electronic angular momenta. Each CSF is a linear combination of multi-electron Slater determinants. That is,

$$\Psi(R) = \sum_{i=1}^N c_i(R)\Phi_i. \quad (2)$$

The Slater determinants in each CSF are built from MOs  $\phi_1(\mathbf{r}), \dots, \phi_M(\mathbf{r})$ . The CSFs in equation (2) depend in general on  $R$  through the MOs, but since our goal will be to minimize this dependence we do not write it explicitly. In a complete active space (CAS) calculation, CSFs are included from every possible configuration of electrons in the orbitals from the active space.

It can be shown that the expectation value of the energy  $\langle H \rangle$  from a CAS-MCSCF wavefunction is invariant to orbital rotation within the active space [20]. In other words,  $\langle H \rangle$  is unchanged if one uses a new set of MOs  $\phi'_i$  related to the old by an arbitrary unitary transformation  $U$  within the active space:

$$\phi'_i = \sum_j U_{ij} \phi_j. \quad (3)$$

This invariance suggests that a strategy for finding the best set of MOs at each  $R$  would be to rotate the initially calculated orbitals so that they are as close as possible to a set of 'reference' orbitals. For scattering applications, as in the present work, the reference orbitals are best determined by calculations in the limit  $R \rightarrow \infty$ . We use the natural orbitals that result from the state-averaged CAS-MCSCF calculation, which may be expressed

$$\phi_i^{(\infty)}(\mathbf{r}) = \sum_j a_{ij}^{(\infty)} g_j(\mathbf{r}), \quad (4)$$

where the  $g_j(\mathbf{r})$  are the normalized atomic basis functions. The simplest approximation to the reference orbitals at a given  $R$  would be to construct MOs using the same expansion coefficients  $a_{ij}^{(\infty)}$ . This set of orbitals is no longer orthonormal, so we symmetrically orthogonalize it [21]. This procedure has been shown [22] to produce the set of orthonormal vectors closest to the original set. It is not necessary to include all the MOs in the symmetric orthogonalization; we included only core orbitals and those in the active space. After implementing this procedure, we may write the reference orbitals as

$$\chi_i(\mathbf{r}) = \sum_j a_{ij}^{(\text{ref})} g_j(\mathbf{r}), \quad (5)$$

where the coefficients  $a_{ij}^{(\text{ref})}$  are easily determined numerically.

The desired rotation of the MOs can be constructed as a sequence of Jacobi rotations by looping over all possible pairs of orbitals in the active space [17]. The basic step is to rotate a pair of MOs so that the new orbitals resemble as closely as possible the corresponding reference orbitals. For the pair  $\phi_i$  and  $\phi_j$ , we find the rotation angle  $\theta$  that minimizes

$$|(\phi_i \cos \theta - \phi_j \sin \theta) - \chi_i|^2 + |(\phi_i \sin \theta + \phi_j \cos \theta) - \chi_j|^2. \quad (6)$$

Since the MOs are normalized, this is equivalent to maximizing

$$f(\theta) = \langle (\phi_i \cos \theta - \phi_j \sin \theta) | \chi_i \rangle + \langle (\phi_i \sin \theta + \phi_j \cos \theta) | \chi_j \rangle, \quad (7)$$

where the inner products signify overlap integrals. This expression differs slightly from the one used by Domcke *et al* [16] and leads to a simpler result. The optimum rotation angle  $\theta$  is determined by

$$\tan \theta = \frac{\langle \phi_i | \chi_j \rangle - \langle \phi_j | \chi_i \rangle}{\langle \phi_i | \chi_i \rangle + \langle \phi_j | \chi_j \rangle}. \quad (8)$$

It is important to check whether changing the sign of one of the rotated orbitals leads to a larger value of  $f(\theta)$ . The rotated MOs determined by this procedure have, in a well defined sense, the desired minimum variation with  $R$ .

Finding an appropriate set of MOs is the first step in determining the diabatic Hamiltonian. The next step is to calculate the full electronic wavefunction, in some degree of approximation. A straightforward approach would be to set up the matrix representation of the electronic Hamiltonian using the CSFs determined for the CAS-MCSCF calculation. However, one would often prefer to implement a better treatment of correlation effects by including additional CSFs.

In 1988, Pacher *et al* [14] presented a method for ‘block diagonalizing’ a large Hamiltonian  $H$  in such a way that a small set of target states is rigorously uncoupled from all other states, without introducing unwanted rotation within the target states. Their method is related to the effective Hamiltonian construction of des Cloizeaux [23]. A key advantage of the results of Pacher *et al* [14] was the simplicity of the numerical prescription. The typical electronic structure calculation involves calculating the lowest few eigenvalues and eigenvectors of a very large sparse matrix (dimension  $10^4$ – $10^6$  when single and double excitations are included). Pacher *et al* [14] determined a diabatic representation of  $H$  in the small set of target states using only the lowest few eigenvectors and eigenvalues of  $H$ , and using only operations involving matrices of the size of the diabatic block desired.

To implement the block diagonalization procedure, one identifies a small set of  $N_\alpha$  CSFs that make the largest contributions to the desired electronic states. Typically, these CSFs are a subset of the CAS-MCSCF configurations, and they are said to define the  $\alpha$  CSFs. All other CSFs, including possibly single and double excitations, define the  $\beta$  set. The dimension of the  $\alpha\alpha$  block ( $N_\alpha$ ) corresponds to the dimension of the diabatic Hamiltonian that will be determined. Using standard techniques [24], one can easily determine the lowest  $N_\alpha$  eigenvalues  $E_1, \dots, E_{N_\alpha}$  and eigenvectors of  $H$ . Using only the  $\alpha\alpha$  block of the eigenvector matrix  $Q$ , one can write the desired diabatic Hamiltonian

$$\mathbf{H}^{\text{diabatic}} = \mathbf{T}^\dagger \mathbf{E} \mathbf{T}, \quad (9)$$

where the dagger denotes the transpose;  $\mathbf{E}$  is the diagonal matrix whose elements are the eigenvalues  $E_1, \dots, E_{N_\alpha}$  and

$$\mathbf{T} = \mathbf{Q}_{\alpha\alpha}^{-1} (\mathbf{Q}_{\alpha\alpha} \mathbf{Q}_{\alpha\alpha}^\dagger)^{1/2}. \quad (10)$$

Because  $\mathbf{T}$  is a unitary transformation within the  $\alpha$  space, the eigenvalues of  $\mathbf{H}^{\text{diabatic}}$  are exactly equal to the set  $E_1, \dots, E_{N_\alpha}$ .

## 2.2. Calculations for $\text{OH}^+$

This section presents details of our application to  $\text{OH}^+$ . All of the jobs were set up as a sequence of electronic structure calculations performed using the GAMESS code [24]. Since Saxon and Liu [9] had mentioned the importance of the first Rydberg orbital, we paid particular attention to the role of the  $\text{O}(2p^3 3s \ ^3\text{S})$  state in the electronic wavefunction. In order to investigate this role, we performed calculations using basis sets with and without the diffuse functions needed to represent the 3s orbital.

Calculation I was performed with the triple zeta valence (TZV) basis set [25], (10s, 6p)/[5s/3p] for O and (5s)/[3s] for H. The oxygen basis was supplemented with two d orbitals with GAMESS’s default exponents, and the hydrogen basis was supplemented with two p orbitals. The exponents are given in table 1. This basis has a total of 35 atomic orbitals. Configurations for the MCSCF calculation were defined by freezing the doubly occupied core orbitals  $1s^2 2s^2$  on oxygen, and including  $2p_z, 2p_x, 2p_y$  and  $1s_{\text{H}}$  in the active space. (The subscript ‘H’ denotes hydrogen.) The state averaged MCSCF was performed by minimizing the energy of the lowest four states with equal weighting. (One of these states had  $^3\Delta$  symmetry.)

For calculation II, we added two diffuse s and two diffuse p basis functions to the oxygen TZV basis of calculation I. The exponents were chosen to provide a good representation of the excited oxygen 3s and 3p orbitals. The asymptotic forms of the orbitals were estimated from the ionization potential of these states. Consideration of the two- and three-Gaussian expansions of STOs by Huzinaga [26] suggested appropriate exponents. The hydrogen basis was enlarged by two diffuse s functions and one more diffuse p function. They were chosen

**Table 1.** Basis set. The (10s, 6p)/[5s, 3p] basis functions for O and the (5s)/[3s] basis functions for H [25] are not shown. The diffuse orbitals included in calculation II but not calculation I are marked with an asterisk.

	Exponent	Contraction coefficient	Diffuse
Oxygen orbitals			
s	0.153 383	1.000	*
s	0.018 117	1.000	*
p	0.073 333	1.000	*
p	0.028 622	0.506 7	*
	0.011 268	0.558 99	
d	2.56	1.000	
d	0.64	1.000	
Hydrogen orbitals			
s	0.036	1.000	*
s	0.014	1.000	*
p	2.228 416	0.325 65	
	0.518 272	0.785 41	
p	0.139 276	1.000	
p	0.032 392	1.000	*

to provide a good representation of 2s and 2p energies. The exponents are given in table 1. This basis has a total of 48 atomic orbitals. The active space for the MCSCF was enlarged to include the 3s orbital, and the state averaging was over the first five states (four  $^3\Sigma^-$  states and one  $^3\Delta$  state, with equal weighting).

The asymptotic reference orbitals were obtained at  $R = 50\,000 a_0$ . We performed the state averaged MCSCF and then determined the natural orbitals by diagonalizing the weighted density matrix. Tests at larger  $R$  confirmed that the orbitals were sufficiently close to their asymptotic limit. At each  $R$ , we determined the MCSCF orbitals and constructed the reference orbitals as discussed in the previous section, and then performed a series of rotations to align the MCSCF orbitals in the active space with the reference orbitals. It was not necessary to include the  $2p_x$  and  $2p_y$  orbitals in this rotation. The orbitals included in the rotation were the  $2p_z$  and  $1s_{\text{H}}$  for calculation I and also the 3s for calculation II. Note that these are only labels; for example, the orbital we denote by 3s has  $\sigma$  symmetry and includes substantial polarization by the oxygen 3p orbital at small values of  $R$ .

After the CAS-MCSCF and orbital rotation at each  $R$ , the next step was to perform a large-scale CI, using all single and double excitations from the multi-reference MCSCF. Finding the lowest few eigenvalues and eigenvectors of the full CI Hamiltonian matrix provides enough information to perform the block diagonalization procedure. In the CI calculation it was important to preserve the overall sign of the MOs produced by the rotation process at each  $R$ . GAMESS normally assigns the overall sign of an MO by choosing the largest atomic orbital coefficient to be positive. We overrode this in the present calculations to avoid discontinuous sign changes as the atomic orbital coefficients varied with  $R$ .

Finally, the CSFs automatically generated by GAMESS were not always the ones preferred to define the  $\alpha$  space for the block diagonalization. It was straightforward to calculate by hand the unitary transformation between the CSFs generated by GAMESS to more physical states, and then to express the matrix  $Q_{\alpha\alpha}$  in these states. This enabled us to achieve the minimum dimension of the  $\alpha\alpha$  block. Table 2 gives the CSFs used to define the  $\alpha$  block of the electronic Hamiltonian for the block diagonalizations. In terms of these CSFs,  $Q_{\alpha\alpha}$  is nearly equal to the identity matrix in the limit  $R \rightarrow \infty$ .

**Table 2.** The expansion of principal CSFs in Slater determinants. The overbar denotes spin down, and frozen core orbitals are omitted.

CSF	Asymptotic configuration	Slater determinant expansion
$\Phi_1$	$O(2p^4\ ^3P) + H^+$	$ 2p_x 2p_y 2p_z \bar{2}p_z $
$\Phi_2$	$O^+(2p^3\ ^4S) + H$	$\sqrt{\frac{1}{12}} 2\bar{p}_x 2p_y 2p_z 1s_H  + \sqrt{\frac{1}{12}} 2p_x \bar{2}p_y 2p_z 1s_H $ $+ \sqrt{\frac{1}{12}} 2p_x 2p_y \bar{2}p_z 1s_H  - \sqrt{\frac{3}{4}} 2p_x 2p_y 2p_z \bar{1}s_H $
$\Phi_3$	$O^+(2p^3\ ^2D) + H$	$\sqrt{\frac{1}{6}} 2\bar{p}_x 2p_y 2p_z 1s_H  + \sqrt{\frac{1}{6}} 2p_x \bar{2}p_y 2p_z 1s_H $ $- \sqrt{\frac{2}{3}} 2p_x 2p_y \bar{2}p_z 1s_H $
$\Phi_4$	$O(2p^3 3s\ ^3S) + H^+$	$\sqrt{\frac{1}{12}} 2\bar{p}_x 2p_y 2p_z 3s  + \sqrt{\frac{1}{12}} 2p_x \bar{2}p_y 2p_z 3s $ $+ \sqrt{\frac{1}{12}} 2p_x 2p_y \bar{2}p_z 3s  - \sqrt{\frac{3}{4}} 2p_x 2p_y 2p_z \bar{3}s $

### 3. Results and discussion

#### 3.1. Diabatic potential curves

Our results show that the coupling among the various  $^3\Sigma^-$  states depends strongly on  $R$ ; an important issue is then how many states to include in the block of diabatic states. Several exploratory calculations were performed, and the results generally indicated that the smaller  $R$ , the larger the value of  $N_\alpha$  needed to ensure that enough states were included. However, there were cases where increasing the value of  $N_\alpha$  led to pitfalls. The situation is also influenced by basis set effects and by the type of scattering calculation anticipated. This section addresses these issues by discussing the results of several calculations with different basis sets and values of  $N_\alpha$ .

Figures 1 and 2 show representative results from several calculations, and more detailed results are tabulated in table 3. Calculation I was performed with  $N_\alpha = 3$ , and calculation II with  $N_\alpha = 2, 3$  and 4. The fourth state corresponds asymptotically to  $O(2p^3 3s\ ^3S) + H^+$ . Because the 3s orbital is included in the active space for calculation II,  $\Phi_4$  in table 2 is optimized to define the fourth CSF of the  $\alpha$  space. Figure 1 shows the diagonal elements  $H_{ii}(R)$ , for several different calculations. All the curves have been shifted so that their asymptotic values match spectroscopic energies. Figure 2 shows the off-diagonal elements. The results for  $N_\alpha = 2$  are the most different from the others. Otherwise, the results of the various calculations are qualitatively similar for both basis sets and for  $N_\alpha = 3$  or 4. Many of the differences can be well understood and are discussed below.

The results for  $N_\alpha = 2$  are different at small  $R$  because more than two CSFs contribute strongly to the electronic wavefunction near the equilibrium value  $R \sim 2 a_0$ . For larger values of  $N_\alpha$ , our results clearly show that  $H_{12}$ ,  $H_{13}$  and  $H_{23}$  are all significant. At least three states should be considered in the region of the attractive well. On the other hand, essentially the same results are obtained asymptotically for  $H_{12}$  using  $N_\alpha = 2$  and 3 with calculation II. Only the results for  $N_\alpha = 3$  are shown in the right panel of figure 2.

An interesting feature of figure 2 is the oscillation in  $H_{23}$  near  $R = 1.5 a_0$  for calculation II ( $N_\alpha = 3$ ). This behaviour reflects interaction with the 3s Rydberg state not explicitly included in the  $\alpha$  space for this calculation. The diabatic curve corresponding to this state ( $H_{44}$ ) crosses the lower curves from calculation II ( $N_\alpha = 4$ ) near  $R \sim 1.5 a_0$  in figure 1. In the region where the third and fourth diabatic curves are very close, it is clearly not adequate to use  $N_\alpha = 3$ . Increasing  $N_\alpha$  to 4 treats the crossing states equally and leads to a smooth  $H_{23}$ . The values

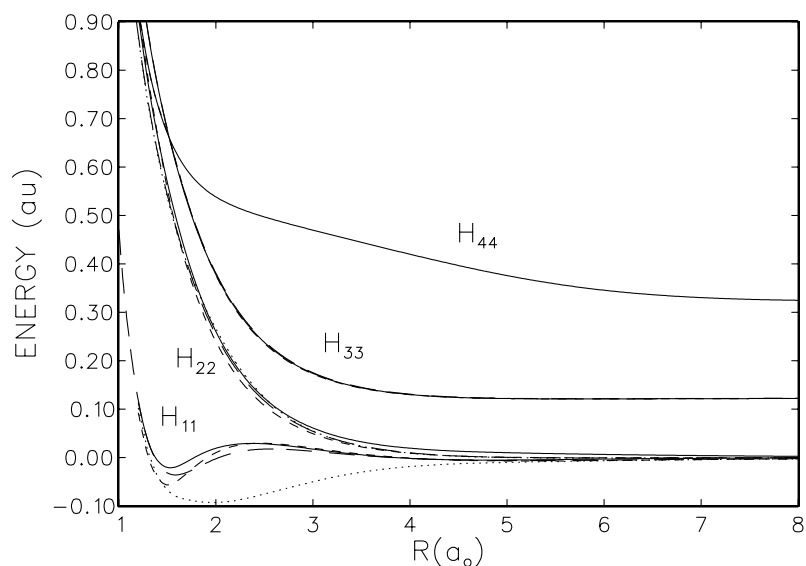


**Figure 1.** Diagonal elements of the diabatic Hamiltonians for several approximations: calculation I with  $N_\alpha = 3$  (—) and calculation II with  $N_\alpha = 2$  (·····),  $N_\alpha = 3$  (- - -) and  $N_\alpha = 4$  (—). The four asymptotic limits correspond, in increasing order, to  $\text{O}(^3\text{P}) + \text{H}^+$ ,  $\text{O}^+(^4\text{S}) + \text{H}$ ,  $\text{O}^+(^2\text{D}) + \text{H}$  and  $\text{O}(^3\text{S}) + \text{H}^+$ .

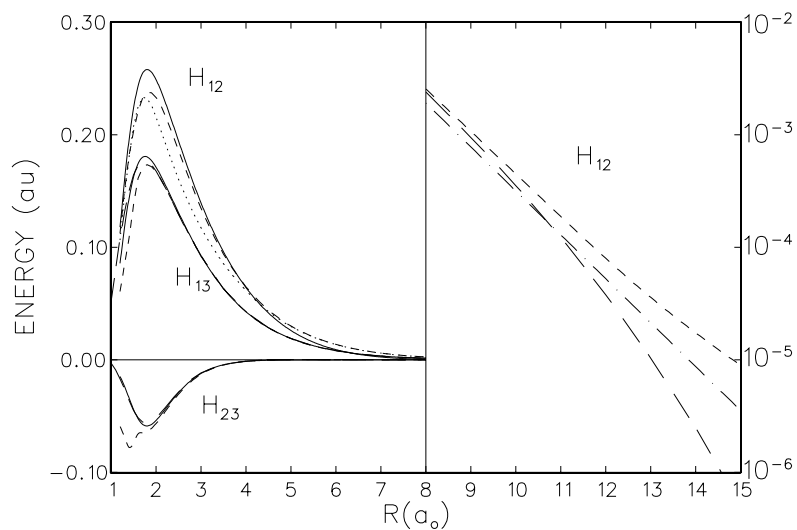


**Figure 2.** Off-diagonal elements of the diabatic Hamiltonians for several approximations: calculation I with  $N_\alpha = 3$  (—) and calculation II with  $N_\alpha = 2$  (·····),  $N_\alpha = 3$  (- - -) and  $N_\alpha = 4$  (—). For comparison, the analytic approximation used by Chambaud *et al* (— · —) is also shown. Note the log scale used for the right panel.

of  $H_{23}(R)$  determined from calculation I with  $N_\alpha = 3$  also do not show oscillations. This is because calculation I does not include sufficiently diffuse basis functions to represent the  $3s$  orbital well. Hence this calculation effectively filters out the fourth state at short range. A few calculations (not shown) were performed at values of  $R$  smaller than  $1 a_0$ ; in this range

**Table 3.** Results of calculation II for  $N_\alpha = 2$  and 3.

$R$	$N_\alpha = 2$			$N_\alpha = 3$					
	$H_{11}$	$H_{12}$	$H_{22}$	$H_{11}$	$H_{12}$	$H_{22}$	$H_{13}$	$H_{23}$	$H_{33}$
1.2	0.102 58	-0.106 37	0.868 02	0.109 13	-0.112 18	0.912 55	-0.060 56	-0.059 16	0.922 52
1.3	0.012 35	-0.146 10	0.732 04	0.025 03	-0.151 24	0.770 80	-0.085 11	-0.069 00	0.804 24
1.4	-0.040 57	-0.180 35	0.624 53	-0.020 63	-0.182 02	0.652 11	-0.108 61	-0.077 83	0.722 36
1.5	-0.068 43	-0.207 31	0.536 58	-0.038 92	-0.202 85	0.544 43	-0.137 58	-0.073 78	0.664 63
1.6	-0.081 20	-0.225 24	0.463 24	-0.037 85	-0.220 75	0.460 38	-0.161 19	-0.065 72	0.597 52
1.7	-0.086 86	-0.233 22	0.401 89	-0.029 19	-0.232 68	0.393 26	-0.170 91	-0.064 91	0.531 44
1.8	-0.090 15	-0.232 37	0.350 21	-0.018 18	-0.237 75	0.336 19	-0.173 49	-0.063 77	0.473 13
1.9	-0.092 29	-0.225 50	0.305 46	-0.007 54	-0.237 37	0.287 49	-0.171 70	-0.060 91	0.422 51
2.0	-0.092 87	-0.215 57	0.265 60	0.001 58	-0.233 07	0.245 92	-0.167 14	-0.056 67	0.378 84
2.1	-0.091 66	-0.204 44	0.229 81	0.008 84	-0.226 08	0.210 42	-0.160 87	-0.051 61	0.341 34
2.2	-0.088 92	-0.193 05	0.197 91	0.014 21	-0.217 31	0.180 12	-0.153 59	-0.046 19	0.309 23
2.3	-0.085 08	-0.181 82	0.169 81	0.017 86	-0.207 43	0.154 26	-0.145 78	-0.040 74	0.281 79
2.4	-0.080 52	-0.170 97	0.145 31	0.020 02	-0.196 92	0.132 19	-0.137 73	-0.035 49	0.258 35
2.5	-0.075 53	-0.160 62	0.124 09	0.020 94	-0.186 14	0.113 32	-0.129 66	-0.030 59	0.238 33
3.0	-0.050 04	-0.117 17	0.055 37	0.015 17	-0.134 73	0.052 28	-0.092 37	-0.012 91	0.173 93
3.5	-0.030 20	-0.085 42	0.023 94	0.005 33	-0.094 06	0.023 26	-0.063 42	-0.004 63	0.143 97
4.0	-0.018 52	-0.061 37	0.009 59	-0.001 71	-0.064 76	0.009 50	-0.042 75	-0.001 29	0.130 22
5.0	-0.010 04	-0.029 76	0.000 50	-0.006 85	-0.030 16	0.000 51	-0.018 85	0.000 22	0.121 88
6.0	-0.006 60	-0.013 62	-0.000 73	-0.006 03	-0.013 66	-0.000 73	-0.008 03	0.000 17	0.121 16
7.0	-0.004 27	-0.005 98	-0.000 50	-0.004 17	-0.005 99	-0.000 50	-0.003 29	0.000 06	0.121 60
8.0	-0.002 76	-0.002 56	-0.000 18	-0.002 74	-0.002 56	-0.000 18	-0.001 29	0.000 02	0.121 98
9.0	-0.001 82	-0.001 08	0.000 03	-0.001 81	-0.001 08	0.000 03	-0.000 48	0.000 00	0.122 21
10.0	-0.001 22	-0.000 45	0.000 16	-0.001 22	-0.000 45	0.000 16	-0.000 16	0.000 00	0.122 35
12.0	-0.000 57	-0.000 08	0.000 29	-0.000 57	-0.000 08	0.000 29	-0.000 01	0.000 00	0.122 48
15.0	-0.000 22	-0.000 01	0.000 35	-0.000 22	-0.000 01	0.000 35	0.000 01	0.000 00	0.122 53
20.0	-0.000 13	0.000 00	0.000 36	-0.000 13	0.000 00	0.000 36	0.000 00	0.000 00	0.122 55
$\infty$	0.000 00	0.000 00	0.000 37	0.000 00	0.000 00	0.000 37	0.000 00	0.000 00	0.122 56

additional excited state curve crossings appear to play a role, and even larger values of  $N_\alpha$  would be necessary.

Changing the basis set has little effect at short range. Calculations I and II using  $N_\alpha = 3$  are very similar for  $R \sim 2-8 a_0$ . A much larger effect at long range is illustrated in the right panel of figure 2, which compares the asymptotic form of  $H_{12}$  obtained from calculations I and II (both with  $N_\alpha = 3$ ) with previous calculations. Chambaud *et al* [10] fit numerical calculations of the appropriate two-electron integrals involving the unperturbed atomic  $2p_z$  and  $1s_H$  orbitals by the analytic form  $H_{12}(R) = 2.548 \exp(-0.899R)$ . Calculation I, which omits diffuse basis functions, roughly agrees with this approximation for  $R \leq 11 a_0$ . The rapid decay of  $H_{12}$  for larger  $R$  is probably an artifact of the poor asymptotic behaviour of the Gaussian basis functions. Calculation II yields significantly larger values of  $H_{12}$  than Chambaud's approximation. Our interpretation of these results is that there is a large  $3s$  component of the lowest-energy  $O + H^+$  state, and that the  $3s$  orbital makes an additional contribution to the charge exchange matrix element.

Further information about the role of the  $3s$  orbital can be obtained by examining the coefficient of CSF  $\Phi_4$ . Figure 3 shows all the elements of the column of  $Q_{\alpha\alpha}$  corresponding asymptotically to CSF  $\Phi_1$ . These elements are the coefficients of the CSFs in the  $\alpha$  space for the eigenvector of the full SDCI Hamiltonian. The strong interaction of  $\Phi_1$  and  $\Phi_2$  is clearly seen near  $R = 4 a_0$  as the corresponding coefficients vary rapidly. (These  $Q_{\alpha\alpha}$  determine the

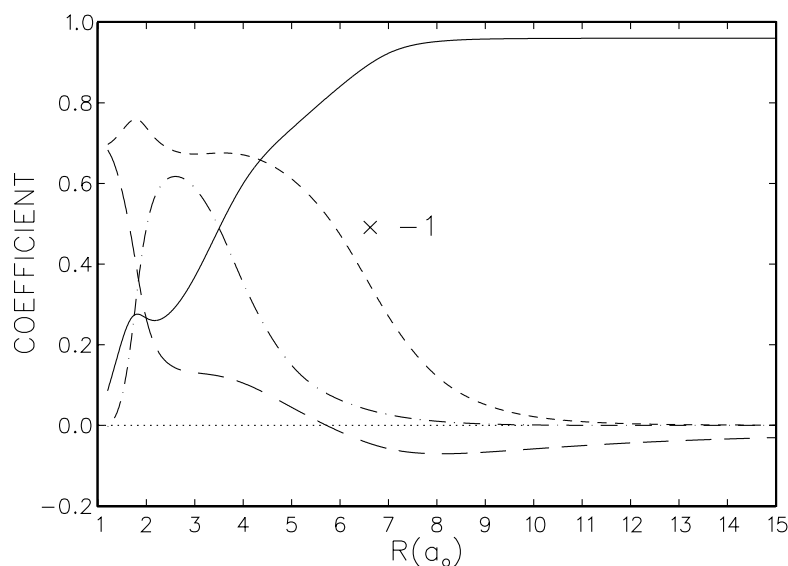


**Figure 3.** Coefficients of the CSFs  $\Phi_1$  (—),  $\Phi_2$  (- - -),  $\Phi_3$  (- · -) and  $\Phi_4$  (— —) in the eigenvector of the full Hamiltonian corresponding asymptotically to the state  $\text{O}(^3\text{P}) + \text{H}^+$ . The coefficient of  $\Phi_2$  has been multiplied by  $-1$ .

diabatic Hamiltonian before the asymptotes are shifted; after shifting, another diagonalization would lead to an avoided crossing at a larger value of  $R$ .) Notice that the other configurations are not negligible. The coefficient of  $\Phi_4$  is particularly large at large  $R$ ; its behaviour can be understood by considering additional matrix elements from calculation II ( $N_\alpha = 4$ ) shown in figure 4.  $H_{14}$  is the coupling between the  $\text{O}(2\text{p}^4\ ^3\text{P})$  level and the  $\text{O}(2\text{p}^3 3\text{s}\ ^3\text{S})$  level induced by the Stark mixing caused by the field of the distant proton.  $H_{14}$  behaves as  $R^{-2}$  asymptotically; in that limit the adiabatic wavefunction for the ground state of  $\text{OH}^+$  is therefore a superposition of  $\Phi_1$  and  $\Phi_4$  as shown in figure 3.

The other coupling terms shown in figure 4 are  $H_{43}$  and  $H_{42}$ .  $H_{42}$  is the charge-exchange coupling between the  $\text{O}(2\text{p}^4\ ^3\text{P}) + \text{H}^+$  configuration (the lowest  $^3\Sigma^-$  state) and the  $\text{O}^+(2\text{p}^3\ ^4\text{S}) + \text{H}$  configuration. Its long range reflects the exponential decay of the diffuse 3s orbital.

The identification of specific diabatic states with different charge states suggests a relation between the diabatic Hamiltonians obtained in calculation II with different values of  $N_\alpha$ . We apply to the  $4 \times 4$  diabatic Hamiltonian the transformation that diagonalizes the  $(H_{11}, H_{14}, H_{41}, H_{44})$  submatrix, since the first and fourth diabatic levels correspond to neutral oxygen plus a proton. Then the new state

$$\Phi'_1 = \cos \theta \Phi_1 + \sin \theta \Phi_4 \quad (11)$$

corresponds to a Stark-mixed neutral oxygen plus a proton, where

$$\tan 2\theta = \frac{2H_{14}}{H_{44} - H_{11}}. \quad (12)$$

$\Phi'_1$  is coupled to the  $\text{O}^+(2\text{p}^3\ ^4\text{S}) + \text{H}$  configuration ( $\Phi_2$ ) by the modified coupling term

$$H'_{12} = H_{12} \cos \theta - H_{24} \sin \theta. \quad (13)$$

Equation (13) illustrates clearly that there are two contributions to the charge-exchange coupling  $H'_{12}$ . Our calculations indicate that in the limit  $R \rightarrow \infty$ , the largest contribution to

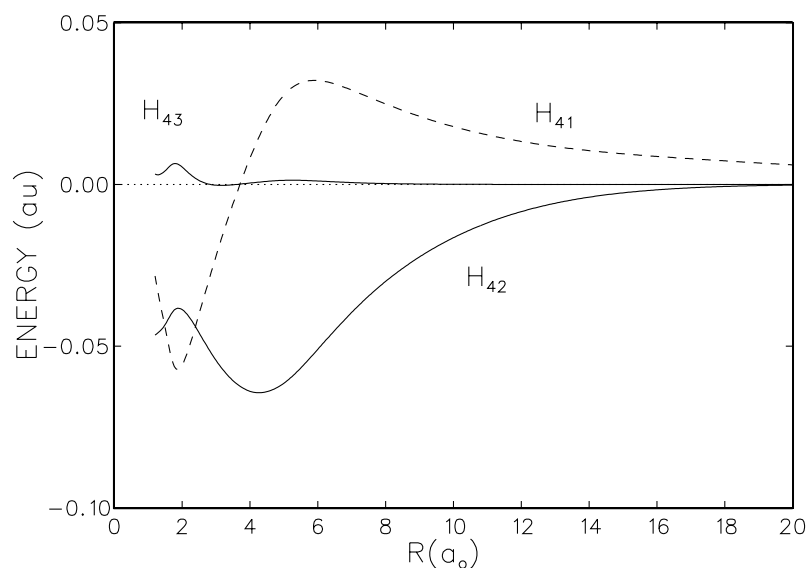


Figure 4. Off-diagonal elements of the  $4 \times 4$  block diagonalization.

$H'_{12}$  originates from the second term on the right-hand side of equation (13). This result makes physical sense. The terms  $H_{12}$  and  $H_{24}$  decay exponentially with  $R$ , but the latter dominates at large  $R$  because of the longer range of the 3s orbital. The mixing angle  $\theta$  is proportional to  $H_{14}$ , which behaves as  $R^{-2}$ . These considerations support the interpretation that at large  $R$  the dominant charge-exchange coupling comes from the product of a small value of  $\sin \theta$  and a relatively large value of  $H_{24}$ . Explicit calculations confirmed that equation (13) is in good agreement with the values of  $H_{12}$  obtained by the block diagonalization of calculation II using either  $N_\alpha = 2$  or 3.

These various calculations lead to several conclusions. First, it is clearly necessary to include very diffuse basis functions. The calculation II basis is superior to the calculation I basis. The extra functions are needed to represent the long-range form of the 2p orbitals and the excited 3s orbital. The question of which value of  $N_\alpha$  to use is less clear: we suspect the answer may depend on what is to be calculated using the diabatic curves.  $N_\alpha = 2$  may be adequate for calculating total cross sections at energies well below the threshold for exciting the  $O^+(^2D)$  state. In this case the block diagonalization method yields a realistic result for  $H_{12}$  at large  $R$  because the Stark mixing of the  $\Phi_1$  and  $\Phi_4$  CSFs is correctly included in the wavefunction for neutral oxygen. A larger value of  $N_\alpha$  might be needed if large-angle differential cross sections are desired, since these results would depend on the coupling at short range, where  $N_\alpha = 2$  is less accurate. Our results suggest that in the region of the attractive well of  $OH^+$  at least three CSFs contribute strongly to the ground state electronic wavefunction. High on the repulsive wall, four or more states may be necessary. As more states are added to the diabatic block, one must treat carefully any situation where two states are strongly coupled. It is necessary to include both states of such a pair for reliable results.

One must also note that for  $N_\alpha \geq 4$ ,  $\Phi_4$  is treated separately, and its effect does not appear in  $H_{12}$ . Hence one must include the  $O(2p^3 3s \ ^3S) + H^+$  channel explicitly in the scattering calculation in order to represent the matrix element for charge exchange correctly asymptotically. At low energies, this channel is deeply closed and hence  $N_\alpha = 2$  or 3 would be preferred.

**Table 4.** Asymptotic energy levels (eV).

	$\text{O}(^3\text{P}) + \text{H}^+$	$\text{O}^+(^4\text{S}) + \text{H}$	$\text{O}^+(^2\text{D}) + \text{H}$	$\text{O}(^3\text{S}) + \text{H}^+$
Spectroscopy	0.0 <sup>a</sup>	0.0100	3.3350 <sup>a</sup>	9.5117
Calculation II	0.0	-0.6134	2.9660	9.0224
Augmented basis	0.0	-0.4266	3.0081	9.2054
Saxon and Liu	0.0	-0.3771	3.1148	
Kimura <i>et al</i>	0.0	-0.46 <sup>b</sup>	3.09 <sup>b</sup>	

<sup>a</sup> Averaged over  $J$  levels.<sup>b</sup> Estimated from a figure.

### 3.2. Accuracy of the potentials and comparison with experiment

As in all *ab initio* calculations, the asymptotic limits of our potential curves do not exactly match spectroscopic energy levels. The details are summarized in table 4. The calculated energies are typically within a few tenths of an electron volt of accurate spectroscopic values [30]. For the  $\text{OH}^+$  system, however, the exact energy difference between the first two levels is less than 0.01 eV. Using the calculated curves without carefully correcting the asymptotes would seriously compromise the scattering calculations. Thresholds would not be correctly represented, and avoided crossings of adiabatic states might occur at unrealistic values of  $R$ .

We have adjusted the diabatic potential curves by shifting each of the diagonal potentials  $H_{ii}(R)$  of the diabatic Hamiltonian by a constant  $\Delta_i$  (independent of  $R$ ) so that the asymptotic energy differences agree with spectroscopic values. The off-diagonal elements, which approach zero asymptotically, are not changed. This adjustment is the simplest that ensures the correct asymptotic limits of the potential curves.

Adjusting the curves means that diagonalizing the ‘shifted’ diabatic Hamiltonian yields modified adiabatic potential curves that need not be exactly the same as those determined by the large-scale quantum chemical calculations. The question arises of how the shifts affect the adiabatic curves. For the ground electronic state, which supports bound vibrational levels, one can calculate the spectroscopic constants and compare them with the corresponding values determined experimentally for  $\text{OH}^+$ .

This comparison is presented in table 5. We first assess the accuracy of the original *ab initio* potentials (calculation II). This calculation yields spectroscopic constants  $R_e$ ,  $D_0$ ,  $\Delta G_{1/2}$ ,  $\Delta G_{3/2}$ ,  $\omega_e$  and  $\omega_e x_e$  for the  $X\ ^3\Sigma^-$  state generally within a few per cent of experimental values [27, 29], but slightly less accurate than those of Saxon and Liu [9]. The results of Kimura *et al* [11] are not included because they were not tabulated. Table 5 also shows the spectroscopic constants of  $\text{OH}^+$  obtained by shifting and then diagonalizing the diabatic Hamiltonians with  $N_\alpha = 2, 3$  and 4. The well depths  $D_e$  and  $D_0$  show improvement as one increases  $N_\alpha$ , but the results for all three values of  $N_\alpha$  are reasonably good.

Assessing the accuracy of the excited  $^3\Sigma^-$  potentials is more difficult since these curves are repulsive, and spectroscopic constants are not defined. To compare our calculations with previous work, we simulated the adiabatic potentials of Saxon and Liu [9] by shifting the asymptotes of our diabatic Hamiltonian to match the asymptotic limits obtained by those authors and then diagonalizing. The simulated repulsive  $2\ ^3\Sigma^-$  curve is about 0.3 eV higher than that of Saxon and Liu for  $R \sim 1.4\text{--}2.4\ a_0$ . In this range, the electronic energy is 6–17 eV higher than the asymptotic value. The simulated  $3\ ^3\Sigma^-$  curve is virtually the same as that of Saxon and Liu.

As a final probe of the reliability of the electronic structure calculations, we performed a few calculations with a larger basis that was augmented by an f basis function for oxygen. The

**Table 5.** Spectroscopic constants for the X  $^3\Sigma^-$  state.

	$R_e$ (Å)	$D_e$ (eV)	$D_0$ (eV)	$\Delta G_{1/2}$ (cm $^{-1}$ )	$\Delta G_{3/2}$ (cm $^{-1}$ )	$\omega_e$ (cm $^{-1}$ )	$\omega_e x_e$ (cm $^{-1}$ )
Present <i>ab initio</i>	1.034	5.406 <sup>a</sup>	5.217 <sup>a</sup>	2923.1	2769.9	3076.3	75.6
2 $\times$ 2 shifted	1.029	5.292	5.101	2963.4	2815.8	3111.0	73.8
3 $\times$ 3 shifted	1.024	5.235	5.042	2981.0	2825.9	3136.1	77.6
4 $\times$ 4 shifted	1.025	5.229	5.037	2973.0	2820.5	3126.7	76.9
Saxon and Liu	1.031	5.358 <sup>a</sup>	5.164 <sup>a</sup>	2942.5	2796.8	3088.1	72.8
Experiment	1.0289 <sup>b</sup>	5.20 <sup>c</sup>	5.007 <sup>d</sup>	2956.34 <sup>b</sup>	2799.3 <sup>b</sup>	3113.37 <sup>b</sup>	78.5 <sup>b</sup>

<sup>a</sup> Determined from O( $^3P$ ) + H $^+$  limit (state 2 in the calculation).

<sup>b</sup> [27].

<sup>c</sup> Estimated from  $D_e = D_0 + \frac{1}{2}\omega_e - \frac{1}{4}\omega_e x_e$  (wavenumber units) [28].

<sup>d</sup> [29].

exponent was  $\alpha = 1.40$ , GAMESS's default value. The results are shown in table 4 in the row labelled 'augmented basis'. The asymptotic energy differences improved by about 0.2 eV, but after shifting the asymptotes the changes in the final diabatic Hamiltonian were much smaller. Near the equilibrium position  $R \sim 2a_0$  the three lowest adiabatic potentials determined by diagonalizing the shifted diabatic potentials changed by only two or three hundredths of an electron volt. This negligible change of the adiabatic potentials supports the validity of our calculations and suggests that our method of shifting the diagonal diabatic potentials provides a reliable correction.

#### 4. Concluding remarks

We have carried out large-scale electronic structure calculations of several  $^3\Sigma^-$  diabatic states and their couplings for the OH $^+$  molecule. The results indicate that the excited O( $2p^33s\ ^3S$ ) state plays an important role in the charge exchange. A small component of this state is mixed with the ground state configuration O( $2p^4\ ^3P$ ) by the Coulomb field of the incident proton. Because the 3s orbital is much longer range than the 2p orbital, it provides the dominant contribution to charge exchange asymptotically. An implication of this result is that the radial coupling matrix elements involving the O( $2p^33s\ ^3S$ ) will be significant.

Our results support the usefulness of the methodology of Pacher *et al* [14] and of Domcke and co-workers [16, 18] for calculating diabatic potential curves. Previous applications of this method have generally addressed conical surface interactions for large molecules, but there is no fundamental difference for diatomics. An important practical consideration is that the dimension of the diabatic Hamiltonian  $N_\alpha$  should be carefully chosen. Different values may be appropriate at different internuclear coordinates, and the value chosen may depend on the ultimate application intended.

The procedure we have used should also be of value for other systems that exhibit closely spaced and strongly interacting adiabatic potential curves. We found that determining a diabatic Hamiltonian, shifting the asymptotes of the diagonal terms to match spectroscopic values and then re-diagonalizing ensured that the coupling between the adiabatic states occurred at the proper distance. The method also led to a small improvement in well depths of the adiabatic potentials.

Further work will involve incorporating these curves in coupled channel calculations of charge exchange and fine-structure mixing in collisions of O with H $^+$  and of O $^+$  with H.

## Acknowledgments

This work was supported by NSF Aeronomy grant no ATM-9810645. JTM was supported by the Research Experiences for Undergraduates programme at Lehigh University. The authors are grateful to DL Huestis and D Talbi for supplying computer programs for finding vibrational energy levels.

## References

- [1] Stebbings R F, Smith A C H and Ehrhardt H 1964 *J. Geophys. Res.* **69** 2349–55
- [2] Black J H and Dalgarno A 1977 *Astrophys. J. Suppl.* **34** 405–23
- [3] Hodges R R Jr and Breig E L 1991 *J. Geophys. Res.* **96** 7697–708
- [4] Reid R H G 1973 *J. Phys. B: At. Mol. Phys.* **6** 2018–39
- [5] Cohen J S and Schneider B I 1974 *J. Chem. Phys.* **61** 3230–9
- [6] Roueff E and Dalgarno A 1988 *Phys. Rev. A* **38** 93–7
- [7] Hickman A P, Medikeri-Naphade M, Chapin C D and Huestis D L 1997 *Phys. Rev. A* **56** 4633–43
- [8] Liu M P D and Verhaegen G 1971 *Int. J. Quantum Chem.* **5** 103–18
- [9] Saxon R P and Liu B 1986 *J. Chem. Phys.* **85** 2099–104
- [10] Chambaud G, Launay J M, Levy B, Millie P, Roueff E and Minh F T 1980 *J. Phys. B: At. Mol. Phys.* **13** 4205–16
- [11] Kimura M, Gu J P, Hirsch G and Buenker R J 1997 *Phys. Rev. A* **55** 2778–85
- [12] Stancil P C, Schultz D R, Kimura M, Gu J P, Hirsch G and Buenker R J 1999 *Astron. Astrophys. Suppl.* **140** 225–36
- [13] Spirko J A and Hickman A P 1999 *Bull. Am. Phys. Soc.* **44** 1102
- [14] Pacher T, Cederbaum L S and Köppel H 1988 *J. Chem. Phys.* **89** 7367–81
- [15] Gadea F X and Pélissier M 1990 *J. Chem. Phys.* **93** 545–51
- [16] Domcke W and Woywood C 1993 *Chem. Phys. Lett.* **216** 362–8
- [17] Ruedenberg K and Atchity G J 1993 *J. Chem. Phys.* **99** 3799–803
- [18] Woywood C, Stengle M, Domcke W, Flöthmann H and Schinke R 1997 *J. Chem. Phys.* **107** 7282
- [19] García V M, Reguero M, Caballol R and Malrieu J P 1997 *Chem. Phys. Lett.* **281** 161–7
- [20] Schmidt M W and Gordon M S 1998 *Ann. Rev. Phys. Chem.* **49** 233–66
- [21] Szabo A and Ostlund N S 1996 *Modern Quantum Chemistry: Introduction to Advanced Electronic Structure Theory* (New York: Dover)
- [22] Carlson B C and Keller J M 1957 *Phys. Rev.* **105** 102–3
- [23] des Cloizeaux J 1960 *Nucl. Phys.* **20** 321–46
- [24] Schmidt M W *et al* 1993 *J. Comput. Chem.* **14** 1347–63
- [25] Dunning T H 1971 *J. Chem. Phys.* **55** 716–23
- [26] Huzinaga S 1965 *J. Chem. Phys.* **42** 1293–302
- [27] Merer A J, Malm D N, Martin R W, Horani M and Rostas J 1975 *Can. J. Phys.* **53** 251–83
- [28] Herzberg G 1989 *Spectra of Diatomic Molecules* (reprint edn) (Malabar, FL: Krieger)
- [29] Helm H, Cosby P C and Huestis D L 1984 *Phys. Rev. A* **30** 851–7
- [30] Moore C E 1993 *Tables of Spectra of Hydrogen, Carbon, Nitrogen, and Oxygen Atoms and Ions* (Boca Raton, FL: Chemical Rubber Company)